Inorganica Chimica Acta, 198–200 (1992) 233–243

Axial ligand bonding in blue copper proteins

Michael D. Lowery and Edward I. Solomon*
Department of Chemistry, Stanford University, Stanford, CA 94305 (USA)

Abstract

Self consistent field-Xα-scattered wave (SCF-Xα-SW) calculations have been used to characterize the bonding between the Cu(II) ion and the axial methionine residue in blue copper proteins. In addition, the interaction of an axial carbonyl oxygen of a glycine residue found at ~3 Å from the copper center in azurins has also been considered. Seven blue copper model sites were constructed to probe various changes in copper coordination and to examine the effects of Zn(II) substituted for Cu(II). It was found that the methionine group covalently binds to the Cu(II) ion site at 2.90 Å with bond strengths calculated to be ~30% that of a 'normal' ligand–metal bond. The carbonyl oxygen atom of a glycine residue was found to have essentially no covalent interaction with the blue copper site. The carbonyl oxygen atom does have a weak ionic attraction to the copper ion which is ~1/4 that of the covalent stabilization of the methionine group. The ligand environment in blue copper proteins is best characterized as four coordinate, with three strong 'in-plane' ligands (two His and Cys) and a weaker axial bond to methionine. Substitution of Cu(II) by Zn(II) leads to a loss of covalency and an increase in the ionic interaction and results in a reasonable metal–glycine bond.

Introduction

The blue copper active site occurs in a large number of proteins including the single copper containing plastocyanins, azurins, stellacyanin and amicyanins, the multicopper containing nitrite and nitrous oxide reductases and in the multicopper oxidases laccase, ceruloplasmin and ascorbic acid oxidase [1]. Blue copper centers are easily distinguished from 'normal' copper sites by their characteristic and exceptionally intense visible absorption bands at 595–625 nm ($\epsilon \sim 3000$–6000 M^{-1} cm^{-1}), their unusually small copper hyperfine coupling constant in the $g_{\|}$ region of the EPR spectrum ($A_{\|} < 70 \times 10^{-4}$ cm^{-1}) and their high redox potential (+184 to +680 mV versus NHE). In proteins where the function of the blue copper site is known, it participates in rapid long-range outer-sphere electron transfer. There has been a great deal of effort focussed on understanding the spectral features and the associated electronic structure of the blue copper site, with the goal of relating the electronic structure properties to the active site reactivity [1a].

The first high-resolution X-ray structure of a blue copper protein was that of poplar plastocyanin (*Populus nigra* var. *italica*) by Colman *et al.* in 1978 [2]. The refined structure [3] showed the coordination geometry at the copper center to consist of two Cu–N_δ(His) bonds at 2.10 and 2.04 Å, a 2.13 Å Cu–S_γ(Cys) bond and a Cu–S_δ(Met) bond at 2.90 Å. Figure 1 shows the ligation at the blue copper center. Since the appearance of the poplar plastocyanin X-ray structure, other high resolution crystal structures for blue copper proteins have been reported. These are: the plastocyanins *Oleander nerium* [4], *Enteromorpha prolifera* [5]; the azurins *Alcaligenes denitrificans* [6], *Pseudomonas denitrificans* [7], *Pseudomonas aeruginosa* [8]; the pseudoazurin *Alcaligenes faecalis* F-6 [9]; and cucumber basic blue protein [10]. In addition, crystal structures of two mutants (His35Gln and His35Leu) of *Pseudomonas aeruginosa*

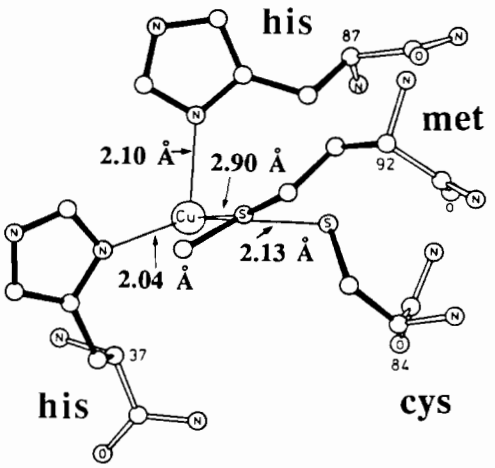

Fig. 1. The blue copper site in poplar plastocyanin [3a].

*Author to whom correspondence should be addressed.

0020-1693/92/$5.00

have recently been reported [11]. In all the X-ray structures determined to date, the blue copper center has been found to have the same four coordinating amino acids in nearly the same geometry as observed in poplar plastocyanin. In the azurins there is an additional carbonyl oxygen atom of a glycine residue at 3.12–2.95 Å from the blue copper site [6, 8a]. Table 1 contains a summary of selected copper–ligand bond distances and angles for poplar plastocyanin [3a] and *Alcaligenes denitrificans* azurin [6a] as these two structures will be used in this study.

Spectroscopic studies [12–14] with poplar plastocyanin single crystals allowed the electronic structure of the blue copper site to be correlated to its geometry. Using single crystal EPR spectroscopy [12], the g tensor orientation was mapped onto the crystallographic coordinates. It was found that the angle between g_z and the Cu–S_δ(Met) bond is ~5° and thus the half-occupied Cu $d_{x^2-y^2}$ orbital, which is perpendicular to g_z, is oriented less than 15° from the remaining three strong 'in plane' ligands (two N_δ(His) and S_γ(Cys)). This results in the blue copper center having effectively an elongated C_{3v} site symmetry with the three-fold z-axis along the Cu–S_δ(Met) bond with significant rhombic distortions due to two histidine and one cysteine ligands.

Polarized single crystal absorption, circular dicroism (CD) and low-temperature magnetic circular dicroism (LTMCD) spectroscopies combined with self consistent field-Xα-scattered wave (SCF-Xα-SW) calculations of the electronic structure of the blue copper site showed that the ~600 nm band was a Cys S → Cu $d_{x^2-y^2}$ charge transfer transition involving the p_π orbital of the thiolate [14]. This had earlier been considered to be a Cys S_σ → Cu charge transfer transition [12]. The change in assignment arises from the strong π-bonding interaction between the copper and the thiolate which rotates the $d_{x^2-y^2}$ orbital such that its lobes bisect the Cu–S_γ(Cys) bond. This leads to a highly anisotropic covalent interaction of the Cu $d_{x^2-y^2}$ orbital with the thiolate which dominates the bonding of the blue copper site. Significant bonding interactions also occur with the two histidine ligands [14]. Thus, these three groups define an 'equatorial' plane about the blue copper center.

TABLE 1. Copper geometry in poplar plastocyanin [3a] and *A. denitrificans* [6a] azurin

Poplar plastocyanin, pH 6.0		*Alcaligenes denitrificans*, pH 5.0	
Ligand–Cu bond lengths (Å)			
Cu–N(His37)	2.04	Cu–N(His46)	2.09
Cu–N(His87)	2.10	Cu–N(His117)	2.00
Cu–S(Cys84)	2.13	Cu–S(Cys112)	2.15
Cu–S(Met92)	2.90	Cu–S(Met121)	3.11
		Cu–O(Gly45)	3.13
Ligand–Cu–ligand bond angles (°)			
N(His37)–Cu–N(His87)	97	N(His46)–Cu–N(His117)	105
N(His37)–Cu–S(Cys84)	132	N(His46)–Cu–S(Cys112)	135
N(His37)–Cu–S(Met92)	85	N(His46)–Cu–S(Met121)	77
N(His87)–Cu–S(Cys84)	123	N(His46)–Cu–O(Gly45)	74
N(His87)–Cu–S(Met92)	103	N(His117)–Cu–S(Cys112)	119
N(Cys84)–Cu–S(Met92)	108	N(His117)–Cu–S(Met121)	96
		N(His117)–Cu–O(Gly45)	80
		S(Cys112)–Cu–S(Met121)	107
		S(Cys112)–Cu–O(Gly45)	104
		S(Met121)–Cu–O(Gly45)	147

There has been some discussion concerning the extent of axial interactions at the blue copper site and thus its coordination number. Extended X-ray absorption fine structure (EXAFS) [15] and Raman [16] experiments failed to find a methionine sulfur–copper interaction. The long 2.9 Å distance of the methionine sulfur–copper determined in the X-ray structure of poplar plastocyanin also led to questions about its significance in bonding [3a]. Thus, some have described the blue copper site as being effectively three coordinate, with copper bound to two histidine nitrogen atoms and the cysteine sulfur atom. On the other hand, for the azurins it has been proposed that the effective geometry at the copper center is best described as five-coordinate (trigonal bipyramidal) with the additional ligand being a carbonyl oxygen atom of a glycine residue at 2.95–3.12 Å from the copper atom in the axial position opposite to the methionine sulfur atom [6, 8a]. The oxygen–copper bond was proposed based on the observation that this was the only polar group in a hydrophobic region of the protein matrix and thus was thought to interact with the positively charged Cu(II) center. Additionally, natural abundance ^{13}C NMR experiments [17] led to the proposal of a copper–amide bond in *Pseudomonas aeruginosa*, however the X-ray crystal structure [8a] found no evidence for an amide nitrogen coordinated to the copper center.

In this work, we use SCF-Xα-SW electronic structure calculations to address the axial bonding interactions of the methionine sulfur and the glycine oxygen atoms with the blue copper center. SCF-Xα-SW calculations probing the methionine interaction have been investigated earlier [13, 14], and it was found that the dimethyl sulfide $4a_1$ orbital was stabilized by interacting with the d_{z^2} orbital of the copper center (the dimethyl sulfide group was used in the calculations as a model for methionine). Here we will expand upon these results and also examine the possibility of a O(Gly)–Cu bond making the copper center in the azurins trigonal bipyramidal. We have constructed several models to probe copper bonding to the methionine sulfur and glycine carbonyl oxygen atoms. As was used in earlier studies [12–14], we have simplified the coordination environment to make the system more amenable for electronic structure calculations: ammonia (NH_3) groups have been used in place of histidine residues, methyl thiolate

(SCH_3^-) for cysteine, dimethyl sulfide ($S(CH_3)_2$) for methionine, and formaldehyde (H_2CO) for glycine*. The effective symmetry of the models is C_s with the copper atom, both sulfur atoms and the carbonyl group on the mirror plane. The models used are shown in Fig. 2 and are briefly described as follows. Models **1–4** are based on the poplar plastocyanin geometry [3]. Model **1** contains the three 'equatorial' ligands (two NH_3 and SCH_3^-). This model serves as a baseline for the changes occurring upon addition of the $S(CH_3)_2$ and H_2CO groups. Model **2** adds the dimethyl sulfide group at the crystallographically observed 2.9 Å S_δ(Met)–Cu bond length found in poplar plastocyanin. Note that the molecular plane of the $S(CH_3)_2$ molecule is oriented perpendicular to the S_γ(Cys)–Cu–S_δ(Met) plane (i.e. the mirror plane). Model **3** probes the effects of moving the dimethyl sulfide group closer to the copper center as is found in the 2.62 Å S_δ(Met)–Cu bond length in the cucumber basic blue structure [18, 10]. Model **4** adds formaldehyde to the plastocyanin site at the 3.12 Å distance found in the azurin crystal structure [6a] and is obtained by adding the H_2CO group to model **2**. Note that the H_2CO molecular plane is rotated 90° relative to the $S(CH_3)_2$ group and is contained within the mirror plane. Structures **5–7** shown in Fig. 2 are based on the *Alcaligenes denitrificans* crystal structure [6a]. The structure of *A. denitrificans* differs from poplar plastocyanin primarily in that the Cu–S_δ(Met) bond length has increased from 2.9 to 3.12 Å and that the carbonyl oxygen of a glycine residue moves from ~4.0 to 3.12 Å from the copper atom. A detailed comparison of the poplar plastocyanin and *A. denitrificans* geometries is presented in Table 1. Model **5** places the five potential ligands at their crystallographically observed distances from the copper center, within the C_s approximation. Model **6** places the H_2CO group at 2.95 Å from the copper site which is the shortest Cu–O(Gly) distance observed to date [8a]. The final model, **7**, evaluates the effect of the metal substitution and replaces the Cu(II) ion in model **5** with Zn(II), but retains the copper geometry.

Using these models, we have evaluated the magnitude of the interactions between the metal atom and the axial dimethyl sulfide and formaldehyde ligands. For covalent mixing of two molecular orbitals to have a net bonding interaction, the antibonding molecular orbital must be either unoccupied or half occupied. Copper(II) has a d^9 electronic configuration and the only 3d orbital that can have a net bonding interaction is the highest-energy half-occupied $d_{x^2-y^2}$ orbital. However, the copper $d_{x^2-y^2}$ orbital is nearly orthogonal to the axial ligands and does not have significant covalent interactions with them. The axial ligand orbitals can interact with the copper d_{z^2} orbital but this level is fully occupied and does not result in a net bonding

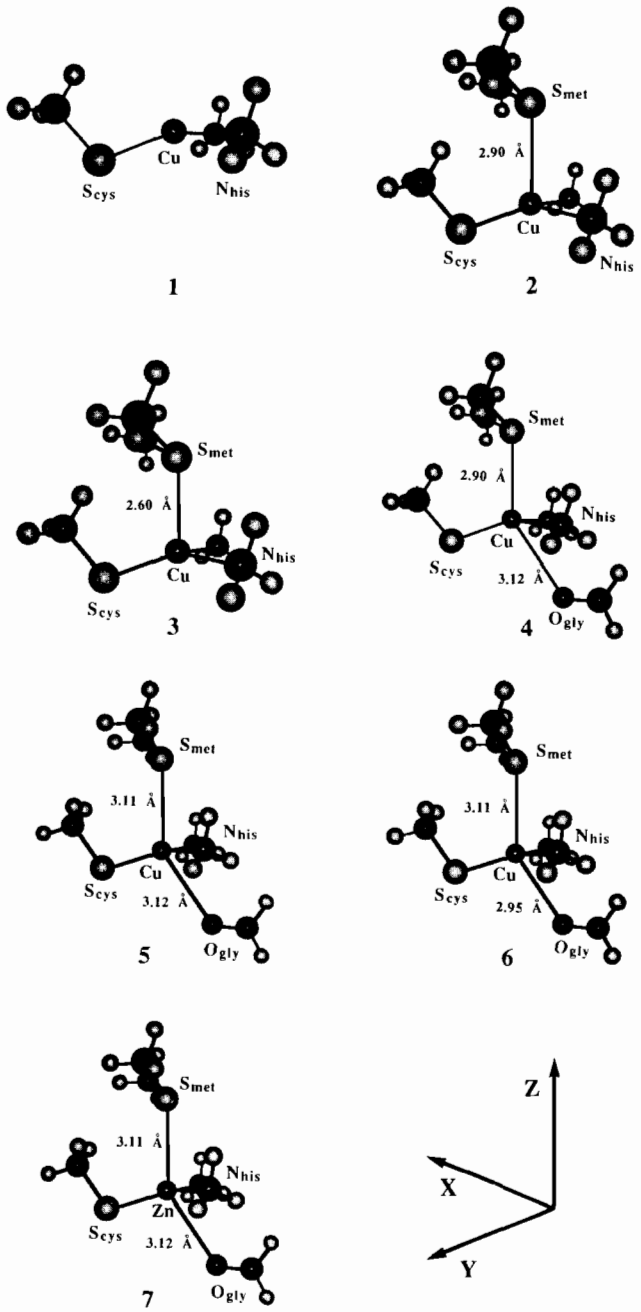

Fig. 2. Blue copper models. Ball-and-stick figures of the seven models used in the electronic structure calculations. See text for a description of the approximations used to construct the models. Each blue copper site is shown with the S_γ(Cys)–Cu–S_δ(Met) bond in the plane of the paper (i.e. the mirror plane in the C_s symmetry of the models).

*Note that a comparison between the C_s(met) (with NH_3 ligation) and C_s(his) (with imidazole ligation) has been made [13]. It was found that substitution of NH_3 for imidazole does not substantially change the character of the ground state wavefunction.

contribution. The primary contribution for bonding in Cu(II) and all of the bonding in Zn(II) involves covalent mixing of the ligand valence orbitals with the unoccupied metal 4s and 4p orbitals. The covalent mixing in these systems can be quantified within the SCF-Xα-SW methodology by determining the amount of metal $3d_{x^2-y^2}$, 4s, and 4p orbital character mixed into the bonding molecular orbitals. In a study of ammonia bonding to ZnO and CuCl surfaces [19] we have used this procedure to evaluate the covalent bond strengths for these d^{10} metal ion systems.

Figure 3 shows contour plots of the highest occupied valence orbitals of dimethyl sulfide and formaldehyde. In dimethyl sulfide, the $2b_2$ and $4a_1$ orbitals (in C_{2v} symmetry with the molecule in the *yz* plane) are primarily localized on the sulfur atom and project towards the copper center in the blue copper site. Level $2b_2$ is the non-bonding pair of electrons which project out from the C–S–C plane (i.e. the $2p_x$ orbital in this coordinate frame). The $4a_1$ orbital is contained in the C–S–C plane (along the two-fold axis) and extends out from the sulfur atom. For H_2CO, the HOMO is level $2b_1$ (in C_{2v} symmetry with the molecule in the *yz* plane) and has the majority of its electron density on the oxygen atom and has mostly $2p_y$ orbital character. These are the orbitals on the axial ligands which are expected to mix with the unoccupied metal 4s and 4p orbitals and will be described using the SCF-Xα-SW electronic structure calculations.

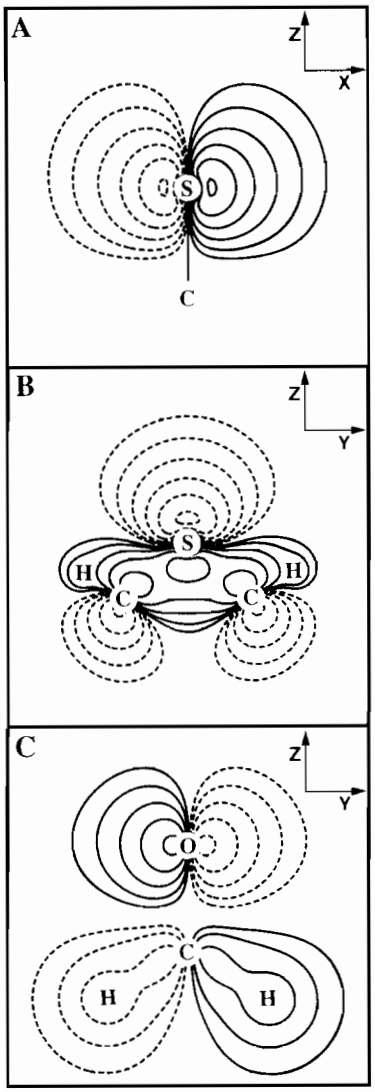

Fig. 3. $S(CH_3)_2$ and H_2CO valence orbital wavefunction plots. (A) The $2b_1$ (HOMO) orbital of $S(CH_3)_2$ in C_{2v} symmetry with the C_2 axis in the *yz* plane. In this coordinate system, the $2b_1$ orbital is p_x in character. In (A) the molecular plane is located perpendicular to the plane of the page and is depicted by the S–C bond shown. (B) The $4a_1$ orbital of $S(CH_3)_2$ shown in the molecular plane. (C) The $2b_2$ HOMO of formaldehyde in C_{2v} symmetry with the C_2 axis in the *yz* plane. For all the figures, the contour levels are at ± 0.01, ± 0.02; ± 0.04; ± 0.08, ± 0.16, ± 0.32 and ± 0.64 (electrons/bohr^3)$^{1/2}$.

Experimental

The 1982 QCPE release [20] of the SCF-Xα-SW program was used for the electronic structure calculations. The code was implemented using a MIPS Fortran compiler on a Digital 3100 computer system. To allow for rapidly evaluating models **1–7**, the C_s(met) approximation to the plastocyanin site [13, 14] (and a similar procedure for the azurin structure) was used in the calculations. In this approximation, the plastocyanin and azurin sites are modeled by $Cu\{S(CH_3)_2\}(SCH_3)(NH_3)_2(H_2CO)]^+$ (or appropriate subsets of this structure) where ammonia replaces the histidine groups, methyl thiolate replaces cysteine, dimethyl sulfide replaces methionine, and formaldehyde replaces glycine. The geometry for the H_2CO molecule was that used by Neumann and Moskowitz [21], and the other ligand geometries were those used in refs. 13 and 14. This approximation for the blue copper site has been found to give results very similar to those obtained with the plastocyanin X-ray structure coordinates [13]. Table 2 gives a summary of the atom coordinates used in the calculations for models **1–7**. Note that the coordinate system has been rotated from that presented in refs. 13 and 14 so that the molecule is positioned in the EPR *g*-tensor frame. This molecular arrangement results in the electronic structure calculations finding the $d_{x^2-y^2}$ orbital as the HOMO.

The atomic exchange parameters, α, were taken from Schwarz [22] and the valence-electron-weighted average of the atomic α values was used for the inner and outer sphere α values. A Watson sphere was used for all the ionic species and its radius was set equal to the outer sphere radius. Calculations were considered converged when the largest deviation of the atomic

TABLE 2. Parameters used in the SCF-Xα-SW calculations[a]

Model	Atom	x	y	z	α	Sphere radius
1	Outer	0.0000	0.0000	0.0000	0.74193	8.2520
	Cu	0.0000	0.0000	0.0000	0.70697	2.9500
	Scys	2.5786	−2.5786	−1.7083	0.72475	2.5000
	Ccys	4.2498	−4.2498	0.6800	0.75928	1.8000
	Hcys a	3.6327	−3.6327	2.4830	0.77725	1.0000
	Hcys b	6.2130	−3.9000	0.4904	0.77725	1.0000
	Hcys b′	3.9000	−6.2130	0.4904	0.77725	1.0000
	Nhis	0.2107	3.9038	0.0504	0.75197	1.9000
	Nhis′	−3.9038	−0.2107	0.0540	0.75197	1.9000
	Hhis a	0.3600	4.5078	1.8488	0.77725	1.0000
	Hhis a′	−4.5078	−0.3600	1.8488	0.77725	1.0000
	Hhis b	−1.3610	4.6341	−0.7356	0.77725	1.0000
	Hhis b′	−4.6341	1.3610	−0.7356	0.77725	1.0000
	Hhis c	1.7357	4.4696	−0.9374	0.77725	1.0000
	Hhis c′	−4.4694	−1.7357	−0.9374	0.77725	1.0000
2 (+1)	Outer	0.0000	0.0000	0.0000	0.74606	10.1346
	Smet	0.3381	−0.3381	5.4650	0.72475	2.2000
	Cmet	3.5440	0.1759	6.6879	0.75928	1.8000
	Cmet′	−0.1759	−3.5440	6.6879	0.75928	1.8000
	Hmet a	3.4392	0.9966	8.5122	0.77725	1.0000
	Hmet a′	−0.9966	−3.4392	8.5122	0.77725	1.0000
	Hmet b	4.5384	1.4057	5.4586	0.77725	1.0000
	Hmet b′	−1.4057	−4.5384	5.4586	0.77725	1.0000
	Hmet c	4.5054	−1.5779	6.7991	0.77725	1.0000
	Hmet c′	1.5779	−4.5054	6.7991	0.77725	1.0000
3 (+1)	Outer	0.0000	0.0000	0.0000	0.74606	9.6019
	Smet	0.3028	−0.3028	4.8946	0.72475	2.2000
	Cmet	3.5087	0.2112	6.1175	0.75928	1.8000
	Cmet′	−0.2112	−3.5087	6.1175	0.75928	1.8000
	Hmet a	3.4039	1.0319	7.9518	0.77725	1.0000
	Hmet a′	−1.0319	−3.4039	7.9418	0.77725	1.0000
	Hmet b	4.5031	1.4410	4.8882	0.77725	1.0000
	Hmet b′	−1.4410	−4.5031	4.8882	0.77725	1.0000
	Hmet c	4.4701	−1.5426	6.2287	0.77725	1.0000
	Hmet c′	1.5426	−4.4701	6.2287	0.77725	1.0000
4 (+2)	Outer	0.0000	0.0000	0.0000	0.74753	10.5571
	Ogly	−2.5709	2.5709	−4.6535	0.74447	1.3700
	Cgly	−4.1848	4.1848	−4.6535	0.75928	1.6000
	Hgly a	−4.9717	4.9717	−2.8619	0.77725	1.1190
	Hgly b	−4.9719	4.9719	−6.4452	0.77725	1.1190
5	Outer	0.0000	0.0000	0.0000	0.74753	10.7567
	Cu	0.0000	0.0000	0.0000	0.70697	2.9500
	Smet	0.3623	−0.3623	5.8556	0.72475	2.2000
	Cmet	3.2224	0.4952	7.4602	0.75928	1.8000
	Cmet′	−0.4952	−3.2224	7.4602	0.75928	1.8000
	Hmet a	3.9436	2.1925	6.6782	0.77725	1.0000
	Hmet a′	−2.1925	−3.9436	6.6782	0.77725	1.0000
	Hmet b	2.8397	0.7670	9.4075	0.77725	1.0000
	Hmet b′	−0.7670	−2.8397	9.4075	0.77725	1.0000
	Hmet c	4.5739	−0.9672	7.2431	0.77725	1.0000
	Hmet c′	0.9672	−4.5739	7.2431	0.77725	1.0000
	Scys	2.6557	−2.6557	−1.5250	0.72475	2.5000
	Ccys	4.1894	−4.1894	1.1441	0.75928	1.8000
	Hcys a	5.5235	−5.5235	0.4712	0.77725	1.0000
	Hcys b	5.1255	−2.8125	2.2578	0.77725	1.0000
	Hcys b′	2.8125	−5.1255	2.2578	0.77725	1.0000
	Nhis	0.5173	3.7943	0.4396	0.75197	1.9000
	Nhis′	−3.7943	−0.5173	0.4396	0.75197	1.9000

(*continued*)

TABLE 2. (*continued*)

Model	Atom	x	y	z	α	Sphere radius
	Hhis a	0.8367	4.1795	2.2619	0.77725	1.0000
	Hhis a′	−4.1795	−0.8367	2.2619	0.77725	1.0000
	Hhis b	−1.0310	4.7120	−0.1363	0.77725	1.0000
	Hhis b′	−4.7120	1.0310	−0.1363	0.77725	1.0000
	Hhis c	1.9999	4.3515	−0.5912	0.77725	1.0000
	Hhis c′	−4.3515	−1.9999	−0.5912	0.77725	1.0000
	Ogly	−2.5709	2.5709	−4.6535	0.74447	1.3700
	Cgly	−4.1848	4.1848	−4.6535	0.75928	1.6000
	Hgly a	−4.9717	4.9717	−2.8619	0.77725	1.1190
	Hgly b	−4.9717	4.9717	−6.4446	0.77725	1.1190
6 (+5)	Outer	0.0000	0.0000	0.0000	0.74753	10.7567
	Ogly	−2.4269	2.4269	−4.3939	0.74447	1.3700
	Cgly	−4.0408	4.0408	−4.3929	0.75928	1.6000
	Hgly a	−4.8277	4.8277	−2.6013	0.77725	1.1190
	Hgly b	−4.8277	4.8277	−6.1845	0.77725	1.1190
7 (+5)	Outer	0.0000	0.0000	0.0000	0.74693	10.7567
	Zn	0.0000	0.0000	0.0000	0.70673	2.4500

[a]All distances are in bohrs (1 bohr = 0.529177 Å). Only new or modified coordinates are given for structures **2**, **3**, **4** and **7**. Structures **2** and **3** are obtained by adding the $S(CH_3)_2$ molecule at 2.90 and 2.60 Å from the Cu atom in structure **1**, respectively. Structure **4** is derived from **2** by adding the H_2CO molecule at 3.12 Å from the Cu atom. Structures **6** and **7** are derived from the azurin coordinates given in **5** by moving the H_2CO to 2.95 Å from the Cu atom and substituting Zn for Cu. Primes are used to designate the second atom of a symmetry equivalent pair. 'Outer' is the outer sphere used in the muffin tin approximation.

potentials between SCF cycles was less than 10^{-4}. This was usually achieved within 500 SCF iterations. The sphere radii for Cu(II), NH_3, $S(CH_3)_2$ and SCH_3^- were those determined by optimizing the ground state wavefunction to the EPR g values found for plastocyanin [14]. The hydrogen radii were fixed at 1.0000 bohr for all atoms except H_2CO, as this radius was found to be optimum in a study by Case and Karplus for copper porphine [23]. The sphere radii for H_2CO used were those determined by Batra and Robaux [24]. The sphere radius for the Zn(II) ion was that used in the study of NH_3 binding to ZnO [19].

Results and analysis

The thioether–copper bond

The objective of these electronic structure calculations is to quantify the bonding changes which occur in the blue copper model complexes upon inclusion of the axial ligands dimethyl sulfide (modeling methionine) and formaldehyde (modeling glycine). The data presented in Table 3 summarize the relevant bonding interactions for models **1**, **2** and **3** (those based on the poplar plastocyanin crystal structure). Model complex **1**, with no axial ligands, serves as a baseline upon which bonding changes occurring upon the addition of dimethyl sulfide can be compared. As has been observed earlier, the HOMO is found to be strongly delocalized onto the equatorial ligands (primarily the Cys sulfur atom) and has ~52% copper $d_{x^2-y^2}$ character*. The percentage of Cu 4s and 4p character found when summed over all the valence molecular orbitals in model **1** is 39.51% Cu 4s and 59.61% Cu 4p. Changes in the %Cu 4s and 4p character upon introduction of the axial ligand, and in particular the % 4s and 4p character mixed into the valence orbitals of the dimethyl sulfide, give a measure of the covalent bonding present with the axial group.

The effects of addition of the $S(CH_3)_2$ group at 2.90 (model **2**) and 2.60 (model **3**) Å from the copper center are also shown in Table 3. The copper d orbital which is most strongly affected by the dimethyl sulfide group is the d_{z^2} orbital. This orbital is directed toward the sulfur atom and overlaps primarily with the dimethyl sulfide $2b_2$ and $4a_1$ orbitals (see Fig. 3). The total amount of d_{z^2} character mixed into the valence orbitals of $S(CH_3)_2$ is found to be 6.47% and 11.46% for Cu–S bond lengths of 2.90 and 2.60 Å, respectively. These data show that there is appreciable covalent interaction between the blue copper site and the dimethyl sulfide group at these distances. This overlap, however, does not imply the presence of a covalent bond between

*Note that the $d_{x^2-y^2}$ character in the HOMO was found to be 42 ± 3% in ref. 14. This was for the C_s(met) blue copper model which included the dimethyl sulfide group.

TABLE 3. Bonding changes in $[Cu(SCH_3)(NH_3)_2]^+$ upon $S(CH_3)_2$ coordination[a]

	1	2		3	
% Cu $d_{x^2-y^2}$ in HOMO	52.44	48.98 (−3.46)		48.86 (−3.58)	
% Cu d_{z^2} in $S(CH_3)_2$ orbitals		6.47		11.46	
	Sum over all valence orbitals	Sum over $S(CH_3)_2$ valence orbitals	Sum over all valence orbitals (change, 2–1)	Sum over $S(CH_3)_2$ valence orbitals	Sum over all valence orbitals (change, 3–1)
% Cu 4s	39.51	1.96	40.30 (0.79)	8.11	41.93 (2.42)
% Cu 4p	59.61	3.07	65.04 (5.43)	4.37	70.14 (10.53)

[a]Values in parentheses give the change in % orbital character relative to model **1**.

the dimethyl sulfide molecule and the blue copper site as the sulfur p and copper d_{z^2} orbitals are fully occupied and cannot lead to a net bonding interaction.

The electronic structure calculations find 48.98% and 48.86% Cu $d_{x^2-y^2}$ character in the HOMO of models **2** and **3**, respectively. This corresponds to a change of $\sim -3.5\%$ in the $d_{x^2-y^2}$ character relative to model **1**, and would imply that there is some delocalization of copper $d_{x^2-y^2}$ character into the $S(CH_3)_2$ valence orbitals. However, inspection of the dimethyl sulfide valence orbitals shows no copper $d_{x^2-y^2}$ character, and the $d_{x^2-y^2}$ mixing does not change on reducing the Cu–S_δ(Met) bond from 2.9 to 2.6 Å. From this, it can be concluded that the dimethyl sulfide group does not participate in covalent bonding with the copper $d_{x^2-y^2}$ orbital. This is reasonable as the $d_{x^2-y^2}$ orbital is oriented in the equatorial plane and does not overlap with axial ligands to any great extent. The $\sim -3.5\%$ change in Cu $d_{x^2-y^2}$ character in the HOMO upon inclusion of the $S(CH_3)_2$ group may arise from differences in repartitioning the electronic charge due to changes in the inter-sphere volume or may result from inductive effects of the dimethyl sulfide group with the equatorial ligands.

The %Cu 4s and 4p orbital character found in models **2** and **3** are presented in the lower half of Table 3. For the dimethyl sulfide group at 2.90 Å from the blue copper site, the electronic structure calculations find a total of 5.03 %Cu 4s and 4p orbital character mixed into the $S(CH_3)_2$ wavefunctions. The level of Cu 4s and 4p orbital mixing into the dimethyl sulfide molecular orbitals closely parallels the total change of 6.22% Cu 4s and 4p character obtained by subtracting the % Cu 4s and 4p character summed over all the valence orbitals for model **2** from that in model **1**. When the dimethyl sulfide molecule is moved to 2.60 Å from the copper center, the covalent interaction increases to a total of 12.48% Cu 4s and 4p orbital character (summed over the $S(CH_3)_2$ orbitals). These results clearly show that the dimethyl sulfide group can covalently bind with the blue copper site at the crystallographically determined Cu–S_δ(Met) distances of 2.90–2.60 Å.

Carbonyl oxygen–copper interaction

Electronic structure calculations which include the formaldehyde molecule were performed in order to probe the possibility of a carbonyl oxygen of a glycine residue coordinating to the blue copper site as has been proposed from the crystallographic analysis of *Alcaligenes denitrificans* [6a] and *Pseudomonas aeruginosa* [8a] azurins. Here we use the electronic structure calculation results for model **2**, which is derived from the poplar plastocyanin structure and does not contain the H_2CO group, as a baseline to judge the effects of addition of the carbonyl oxygen to the copper coordination sphere. A summary of the results obtained is presented in Table 4.

Model **4** is obtained by adding the H_2CO molecule to model complex **2** with a Cu–O distance of 3.12 Å and a Cu–O–C bond angle of 128°. The distance and angle used here is the average of the two crystallographically independent values determined by Baker [6a] for the carbonyl oxygen of glycine 45 in *Alcaligenes denitrificans*. As was observed for $S(CH_3)_2$ above, the H_2CO molecule does not interact appreciably with the half-occupied $d_{x^2-y^2}$ orbital. The 2.42% decrease in the $d_{x^2-y^2}$ HOMO character does not appear in the H_2CO valence orbitals. The H_2CO molecule also shows much less interaction with the d_{z^2} orbital as only 1.24% d_{z^2} character is mixed into the formaldehyde molecular orbitals. Of greater importance is the % Cu 4s and 4p character mixed into the formaldehyde valence orbitals. Unlike $S(CH_3)_2$, H_2CO has very little interaction with the blue copper center as a total of only 0.97% Cu 4s and 4p character is present in the H_2CO valence orbitals.

TABLE 4. Bonding changes in $[Cu(SCH_3)(NH_3)_2\{S(CH_3)_2\}]^+$ upon H_2CO coordination[a]

	2	4		5		6	
% Cu $d_{x^2-y^2}$ in HOMO	48.98	46.56 (−2.42)		43.31 (−5.67)		43.92 (−6.06)	
% Cu d_{z^2} in H_2CO orbitals		1.24		0.31		0.52	
	Sum over all valence orbitals	Sum over H_2CO valence orbitals	Sum over all valence orbitals (change, 4–2)	Sum over H_2CO valence orbitals	Sum over all valence orbitals (change, 5–2)	Sum over H_2CO valence orbitals	Sum over all valence orbitals (change, 6–2)
% Cu 4s	40.30	0.62	41.30 (1.00)	0.02	41.17 (0.87)	0.04	41.18 (0.88)
% Cu 4p	65.04	0.35	66.34 (1.30)	0.18	63.96 (−1.08)	0.34	64.41 (−0.63)

[a]Values in parentheses give the change in % orbital character relative to model **2**.

To insure an accurate assessment of the carbonyl oxygen–copper interaction, models **5** and **6** were constructed. These models are based on the X-ray structure of *Alcaligenes denitrificans* azurin [6a]. The formaldehyde molecule is positioned 3.12 Å from the blue copper site in model **5**, while model **6** incorporates the shorter 2.95 Å Cu–O(Gly) bond length observed in *Pseudomonas aeruginosa* azurin [8a], but maintains the *A. denitrificans* geometry for the remaining ligands. The electronic structure calculation results for these models are presented below.

As seen in Table 4, the amount of Cu d_{z^2} character mixed into the H_2CO valence orbitals is very small; 0.31% and 0.52% for models **5** and **6**, respectively. There is very little covalent interaction of the carbonyl oxygen $2b_1$ orbital with the copper d_{z^2} orbital (see Fig. 3 for the $2b_1$ orbital orientation). Mixing of the H_2CO valence orbitals with the Cu $d_{x^2-y^2}$ orbital is also negligible. The SCF-Xα-SW calculations find essentially no copper $d_{x^2-y^2}$ character mixed into the formaldehyde molecular orbitals. The $\sim -5.75\%$ change in Cu $d_{x^2-y^2}$ character in models **5** and **6** results from slight geometry changes between the plastocyanin (model **2**) and azurin sites (see Table 1). Inspection of Table 4 shows that in the azurin geometry there is almost no Cu 4s and 4p mixing with the H_2CO valence orbitals. The total change in % Cu 4s and 4p character upon addition of the H_2CO group is 0.20 and 0.38 for **5** and **6**, respectively.

Electronic structure calculations using the azurin geometry with Zn(II) substituted for Cu(II) have been performed (i.e. model **7**). A comparison of the results obtained for $S(CH_3)_2$ and H_2CO binding to the Zn(II) site with those obtained for Cu(II) is given in Table 5. Note that in the azurin geometry the $S(CH_3)_2$ group is 3.12 Å from the blue copper site (the methionine sulfur is 2.90 Å in poplar plastocyanin). However, even at the greater bond length, the dimethyl sulfide group loses only 0.51% Cu 4s and 4p character (model **5** compared to model **2**). Upon metal substitution, the amount of 4s and 4p metal character drops by ~50% for $S(CH_3)_2$, and remains near zero for H_2CO. When summed over the valence orbitals of all the ligands, the Zn(II) ion loses about 20% 4s and 4p bonding character when compared to the Cu(II) site. The data in Table 5 show that the Zn(II) site is much less covalent in its interactions with the blue copper ligands than is the Cu(II) ion.

Discussion

SCF-Xα-SW electronic structure calculations have been used to determine the covalent interaction between the dimethyl sulfide molecule and the blue copper center of poplar plastocyanin. Upon addition of the $S(CH_3)_2$ group at 2.90 Å from the copper (model **2**), the amount of Cu 4s and 4p orbital character mixed into the dimethyl sulfide $2b_2$ and $4a_1$ orbitals was found to be ~5%. To quantify this covalent interaction, the %Cu 4s and 4p character for 'normal' ligand is needed as a reference. To estimate a 'normal' bond, we use the SCF-Xα-SW results for the ammonia–copper bonds in model **2** and also results for ammonia coordinated to CuCl(111) surfaces [19]. The %Cu 4s and 4p character mixed into the ammonia valence orbitals in model **2** is found to be 17.6 (per NH_3 group) and 16.4 for NH_3 coordinated to the Cu(I) surface site in CuCl. Therefore, a 'normal' bond has ~17% Cu 4s and 4p character mixed into the ligand valence orbitals. Relative to this, the 5% Cu 4s and 4p mixing found for $S(CH_3)_2$ in model **2** represents approximately 30% that of a 'normal' bond. Moving the dimethyl sulfide to 2.6 Å from the blue copper site increases the Cu–S_δ(Met) covalent bonding interaction to ~70% that of a 'normal' bond (~12.5% Cu 4s and 4p character for model **3**). Heat

TABLE 5. Effect of metal substitution on bonding in azurin[a]

	Sum over $S(CH_3)_2$ valence orbitals		Sum over H_2CO valence orbitals		Sum over all valence orbitals	
	% 4s	% 4p	% 4s	% 4p	% 4s	% 4p
5 [Cu(II)]	1.12	3.40	0.02	0.18	41.17	63.96
7 [Zn(II)]	0.49	1.99	0.13	0.09	42.01	42.49
Difference (**7–5**)	−0.63	−1.41	0.11	−0.09	0.84	−21.47

[a]The azurin geometry is based on the X-ray structure of *Alcaligenes denitrificans* [6a]. Note here that the $S(CH_3)_2$ group is 3.12 Å from the metal center (vs. 2.90 Å in poplar plastocyanin) and this results in a loss of −0.51% 4s and 4p character from that given for model **2** in Table 3 (5.03% 4s and 4p).

of adsorption studies [19] of NH_3 chemisorbed to CuCl(111) surfaces found the NH_3–Cu(I) bond strength to be 24±3 kcal/mol. This gives a crude estimate of the dimethyl sulfide–Cu bond strength of approximately 7 kcal/mol for model **2** and 17 kcal/mol for model **3**. Clearly these data show that there is a covalent bond between the dimethyl sulfide group and the blue copper site over the bond distance range of 2.9–2.6 Å. This covalent interaction is depicted in the contour plot presented in Fig. 4 which shows the electron density for model **2** summed over the $S(CH_3)_2$ valence orbitals. Note the substantial electron density bridging the sulfur and copper centers.

Coordination of the carbonyl oxygen atom of formaldehyde at 3.12 Å from the blue copper site was found to have very little (<1% for models **5** and **6**) copper orbital mixing into the H_2CO valence orbital wavefunctions. As shown in Table 4, bringing the H_2CO group to its closest observed distance (2.95 Å) still provided negligible interaction with the Cu 4s and 4p orbitals. The magnitude of the copper 4s and 4p character mixed into the formaldehyde orbitals is less than 10% of that observed for dimethyl sulfide binding to the blue copper site at a comparable distance. An electron density contour plot summed over the H_2CO valence orbitals is presented in Fig. 5. The contour shows that the electron density remains localized on the H_2CO molecule with negligible covalent interaction between the copper and oxygen atoms.

The covalent stabilization energy (W_{cov}) between two molecular orbitals A and B can be approximated by:

$$W_{cov} = -(H_{AB})^2/\Delta E \quad (1)$$

where $H_{AB} = \langle A|H|B\rangle$ is the resonance integral and ΔE is the energy difference between the two orbitals. The magnitude of the resonance integral depends on orbital overlap. The apparent lack of covalent interaction of the blue copper site with the carbonyl oxygen atom at 2.95–3.12 Å, while the $S(CH_3)_2$ group has a modest covalent interaction at approximately the same bond lengths, can be rationalized by comparing the 2p and 3p orbital radial distribution functions [25] for oxygen and sulfur. As seen in Fig. 6, sulfur has far greater radial extent and therefore greater overlap with the copper 4s and 4p orbitals at the 2.6–3.12 Å bond lengths found in the blue copper site.

In addition to the covalent bond interactions discussed above, there can also be ionic contributions to bonding. Both dimethyl sulfide and formaldehyde have appre-

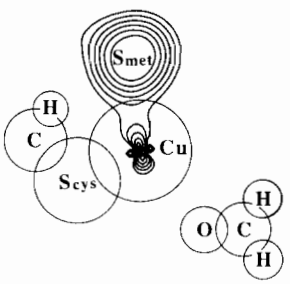

Fig. 4. The methionine–copper bond. Electron density contour plot summed over the valence orbitals of $S(CH_3)_2$ depicting the covalent interaction of the methionine sulfur atom with the blue copper site calculated using the geometry of model **2**. The plot is shown in the S(Cys)–Cu–S(Met) plane (i.e. the C_s plane). The atoms contained on the mirror plane are outlined with the atomic sphere radii used in the SCF-Xα-SW calculations. Contour lines are drawn at 0.005, 0.01, 0.02, 0.04, 0.08, 0.16 and 0.32 electrons/bohr^3.

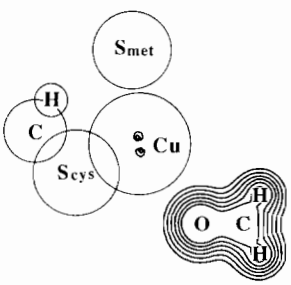

Fig. 5. The carbonyl oxygen–copper interaction. Electron density contour plot summed over the valence levels of H_2CO depicting the covalent interaction of the carbonyl oxygen atom with the blue copper site calculated using the geometry given for model **4**. The plot is shown in the S(Cys)–Cu–S(Met) plane (i.e. the C_s plane). The atoms contained on the mirror plane are outlined with the atomic sphere radii used in the SCF-Xα-SW calculations. Contour lines are drawn at 0.005, 0.01, 0.02, 0.04, 0.08, 0.16 and 0.32 electrons/bohr^3.

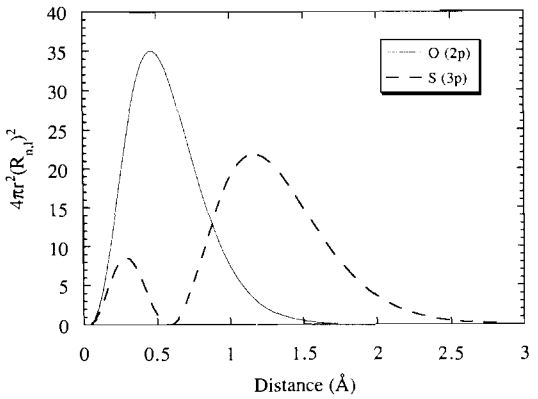

Fig. 6. Plot of the oxygen 2p and sulfur 3p radial distribution functions. Z_{eff} values were calculated using Slater's rules [25] (Z_{eff}=4.55 for O(2p) and 5.45 for S(3p)).

ciable dipole moments of 1.50 and 2.33 D, respectively [26]. These dipole moments can interact with the positive charge of the Cu(II) ion and stabilize the complex. The electrostatic potential energy (W_{el}) for this interaction can be approximated using a point-dipole model [27]

$$W_{el}=Z_{eff}\mu(\cos\theta)/4\pi\epsilon_0\epsilon r^2 \quad (2)$$

where Z_{eff} is the effective charge on the metal ion, μ is the ligand dipole moment, θ is the angle between the midpoint of the dipole and the metal ion, ϵ_0 is the permittivity of a vacuum, ϵ is the dielectric constant in the neighborhood of the blue copper center, and r^2 is the distance from the midpoint of the molecular dipole to the metal ion site. In eqn. (2), the Z_{eff} and ϵ values are difficult to determine unambiguously. A Z_{eff} value of 0.34 was obtained from SCF-Xα-SW calculations of model **2** using the Norman sphere radii [28] and defines a lower limit for the Cu(II) charge as it is known that the Norman radii tend to overestimate covalency in transition metal systems [14, 29]. A reasonable estimate for Z_{eff} of the copper ion in the highly covalent blue copper site is ~0.5*. Approximate values for the dielectric constant in the hydrophobic region about the axial ligands are 2–10. For model **2** using Z_{eff}=0.5 and ϵ=2, an upper limit for the electrostatic attraction energy between Cu(II) and the axial ligands is roughly calculated to be ~1.8 kcal/mol for H_2CO and ~0.8 kcal/mol for $S(CH_3)_2$. Comparison of the ionic potential energy to the covalent term calculated for the Cu–S(Met) bond of model **2** estimates the Cu(II)–H_2CO interaction to be about 1/4 that of the covalent bond strength of the dimethyl sulfide group. Note that for comparable metal charges and dielectric screening values, the H_2CO molecule has approximately twice the electrostatic interaction with the metal center as does the $S(CH_3)_2$ group.

Recently, an X-ray structure of Zn substituted *Pseudomonas aeruginosa* azurin has been determined [30]. The bond lengths observed are S_δ(Met)–Cu=3.30 Å and O(Gly)–Cu=2.32 Å. Results of SCF-Xα-SW calculations for the Zn(II) substituted azurin site presented in Table 5 show that Zn(II) is less covalent than Cu(II) which results in greater orbital contraction and a higher effective nuclear charge on the Zn(II) ion. Previous electronic structure calculations [19] of ammonia bonding to the Zn(II) sites on a ZnO(0001) surface found $Z_{eff}\approx 1.0$. The calculations reported here on the zinc substituted azurin site also indicate that Z_{eff} has increased by a factor of 2 relative to the copper site. Using this Z_{eff} for the zinc ion, and an ϵ of 2 gives an attractive ionic potential of 3.5 kcal/mol for H_2CO at a distance of 3.12 Å. These findings can be used to rationalize the structure changes in zinc substituted azurin in that (i) the covalent interaction of the methionine sulfur with the Zn(II) site is predicted to be reduced by ~50% relative to the copper site and (ii) the carbonyl oxygen atom at 3.12 Å has a factor of 2 greater ionic interaction with the Zn(II) ion and this will increase as the length of the bond decreases ($\alpha 1/r^2$). In Zn(II) substituted azurin, the O(Gly)–Zn bond length should decrease due to increased ionic attraction while the S_δ(Met)–Zn bond length should increase due to loss of covalency.

In conclusion, the electronic structure calculations show that the methionine sulfur atom at 2.90 Å from the blue copper site does have a covalent interaction with ~30% the strength of a 'normal' copper bond and becomes much stronger as the S_δ(Met)–Cu bond length decreases to 2.60 Å (~70% of a 'normal' Cu–ligand bond). The carbonyl oxygen atom of the glycine residue at 3.12 Å from the blue copper site does not have an appreciable covalent interaction with the copper center. The glycine oxygen atom does, however, have an ionic attraction to the positively charged metal center. Comparison of the relative bond strength contributions finds the covalent contribution to bonding of the methionine group is ~4 times as effective as the ionic attraction of the glycine oxygen atom to Cu(II). The blue copper site is best described as being four coordinate with three strong 'in-plane' ligands and a weaker axial methionine sulfur bond. The Zn(II) substituted azurin site is found to have reduced covalency and stronger ionic contributions to bonding which would shift of the Zn(II) ion away from the methionine sulfur and towards the carbonyl oxygen atom.

*SCF-Xα-SW calculations adjusted to the PES spectrum of NH_3 coordinated to a CuCl(111) surface [19] give +0.5 C for the copper charge.

Acknowledgement

This work was supported by NFS Grant CHEM 8919687.

References

1 (a) E. I. Solomon, M. J. Baldwin and M. D. Lowery, *Chem. Rev.*, in press; (b) E. T. Adman, in C. B. Anfinsen, J. T. Edsall, F. M. Richards and D. S. Eisenberg (eds.), *Advances in Protein Chemistry,* Vol. 42, Academic Press, San Diego, 1991, p. 145; (c) A. G. Sykes, *Struc. Bonding (Berlin), 75* (1991) 175; (d) O. Farver and I. Pecht, *Coord. Chem. Rev., 94* (1989) 17; (e) E. I. Solomon, K. W. Penfield and D. E. Wilcox, *Struc. Bonding (Berlin), 53* (1983) 3; (f) H. B. Gray and E. I. Solomon, in T. G. Spiro (ed.), *Copper Proteins,* Wiley–Interscience, New York, 1981, Ch. 1.

2 P. M. Colman, H. C. Freeman, J. M. Guss, M. Murata, V. A. Norris, J. A. M. Ramshaw and M. P. Venkatappa, *Nature (London), 272* (1978) 319.

3 (a) J. M. Guss and H. C. Freeman, *J. Mol. Biol., 169* (1983) 521; (b) J. M. Guss, P. R. Harrowell, M. Murata, V. A. Norris and H. C. Freeman, *J. Mol. Biol., 192* (1986) 361.

4 H. Tong, *Ph.D. Dissertation,* University of Sydney, Sydney, Australia, 1991.

5 C. A. Collyer, J. M. Guss, Y. Sugimura, F. Yoshizaki and H. C. Freeman, *J. Mol. Biol., 211* (1990) 617.

6 (a) E. N. Baker, *J. Mol. Biol., 203* (1988) 1071; (b) G. E. Norris, B. F. Anderson and E. N. Baker, *J. Am. Chem. Soc., 108* (1986) 2784.

7 Z. R. Korszun, *J. Mol. Biol., 196* (1987) 413.

8 (a) H. Nar, A. Messerschmidt, R. Huber, M. van de Kamp and G. W. Canters, *J. Mol. Biol., 221* (1991) 765; (b) E. T. Adman and L. H. Jensen, *Isr. J. Chem., 21* (1981) 8.

9 E. T. Adman, S. Turley, R. Bramson, K. Petratos, D. Banner, D. Tsernoglou, T. Beppu and H. Watanabe, *J. Biol. Chem., 264* (1989) 87.

10 J. M. Guss, E. A. Merritt, R. P. Phizackerley, B. Hedman, M. Murata, K. O. Hodgson and H. C. Freeman, *Science, 241* (1988) 806.

11 H. Nar, A. Messerschmidt, R. Huber, M. van de Kamp and G. W. Canters, *J. Mol. Biol., 218* (1991) 427.

12 K. W. Penfield, R. R. Gay, R. S. Himmelwright, N. C. Eickman, V. A. Norris, H. C. Freeman and E. I. Solomon, *J. Am. Chem. Soc., 103* (1981) 4382.

13 K. W. Penfield, A. A. Gewirth and E. I. Solomon, *J. Am. Chem. Soc., 107* (1985) 4519.

14 A. A. Gewirth and E. I. Solomon, *J. Am. Chem. Soc., 110* (1988) 3811.

15 R. A. Scott, J. E. Hahn, S. Doniach, H. C. Freeman and K. O. Hodgson, *J. Am. Chem. Soc., 104* (1982) 5364.

16 T. J. Thamann, P. Frank, L. J. Willis and T. M. Loehr, *Proc. Natl. Acad. Sci. U.S.A., 79* (1982) 6396.

17 K. Ugurbil, R. S. Norton, A. Allerhand and R. Bersohn, *Biochemistry, 16* (1977) 886.

18 Refined crystal structure parameters for several proteins have been reported, see J. Han, E. T. Adman, T. Beppu, R. Codd, H. C. Freeman, L. Huq, T. M. Loehr and J. Sanders-Loehr, *Biochemistry, 30* (1991) 10904.

19 J. Lin, P. M. Jones, M. D. Lowery, R. R. Gay, S. L. Cohen and E. I. Solomon, *Inorg. Chem., 31* (1992) 686.

20 (a) J. C. Slater and K. H. Johnson, *Phys. Rev. B, 5* (1972) 844; (b) K. H. Johnson, *Adv. Quantum Chem., 7* (1973) 143; (c) K. H. Johnson, J. G. Norman, Jr. and J. W. D. Connolly, in F. Herman, A. D. McLean and R. K. Nesbet (eds.), *Computational Methods for Large Molecules and Localized States In Solids,* Plenum, New York, 1973, p. 161; (d) F. Herman, A. R. Williams and K. H. Johnson, *J. Chem. Phys., 61* (1974) 3508; (e) J. C. Slater, *The Self-Consistent Field for Molecules and Solids: Quantum Theory of Molecules and Solids,* Vol. 4, McGraw-Hill, New York, 1974; (f) J. W. D. Connolly, in G. A. Segal (ed.), *Modern Theoretical Chemistry,* Vol. 7, Plenum, New York, 1977, p. 105; (g) D. A. Case and C. Y. Yang, *Int. J. Quantum Chem., 18* (1980) 1091; (h) D. A. Case, *Ann. Rev. Phys. Chem., 33* (1982) 151.

21 D. B. Neumann and J. W. Moskowitz, *J. Chem. Phys., 50* (1969) 2216.

22 K. Schwarz, *Phys. Rev. B, 5* (1972) 2466.

23 D. A. Case and M. Karplus, *J. Am. Chem. Soc., 99* (1977) 6182.

24 I. P. Batra and O. Robaux, *Chem. Phys. Lett., 28* (1974) 529.

25 B. E. Douglas, D. H. McDaniel and J. J. Alexander, *Concepts and Models of Inorganic Chemistry,* Wiley, New York, 2nd edn., 1983, pp. 13 and 32.

26 R. C. Weast (ed.), *CRC Handbook of Chemistry and Physics,* CRC Press, Cranwood Parkway, Cleveland, OH, 56th edn., 1975, p. E64.

27 P. W. Atkins, *Physical Chemistry,* W. H. Freeman, New York, 4th edn., 1990, p. 655.

28 J. G. Norman Jr., *Mol. Phys., 31* (1976) 1191.

29 (a) A. A. Gewirth, S. L. Cohen, H. J. Schugar and E. I. Solomon, *Inorg. Chem., 26* (1987) 1133; (b) S. V. Didziulis, S. L. Cohen, A. A. Gewirth and E. I. Solomon, *J. Am. Chem. Soc., 110* (1988) 250.

30 G. W. Canters, personal communication.